Analysis of MEMS Based Earthquake Instrument for Nuclear Power Plant

Md. Mehedi HASAN[1], and Jae Cheon JUNG[1]

[1]Department of NPP, KEPCO International Nuclear Graduate School (KINGS), 658-91 Haemajj-ro, Seosaeng-myeon, Ulju-gun, Ulsan 689-882, Republic of Korea, E-mail: mehediapece@yahoo.com, jcjung@kings.ac.kr

Abstract: This work explores an analysis of Micro Electro Mechanical System (MEMS) earthquake instrument which can be used for seismic monitoring in the nuclear power plant. Conventional geophone based seismic instruments suffer significant reduction in recorded velocity-domain amplitudes below their natural frequency. MEMS accelerometers can record to fractions of 1 Hz without any relative reduction in acceleration amplitudes. Firstly, mathematical transfer function models of conventional geophone, MEMS, servo acceleration with feedback loop, and force balanced acceleration using pendulum type accelerometer are elicited. Then the dynamic behaviors of those instruments are assessed due to the effects of transfer function on frequency contents using MATLAB program. MEMS based digital accelerometers provide a broadband linear response (DC to 800 Hz) and very low distortion. A new MEMS based earthquake instrumentation consisting FPGA data processing system is conceptually designed, and synthesized. Ground motion information recorded by the seismic measuring instrument can be observed promptly after an earthquake as Operating Basis Earthquake (OBE), and Safe Shutdown Earthquake (SSE) levels at nuclear power plant to avoid seismic issues. The system can ensure more availability of the plant confirming integrity of the structure, system, and components.

Keywords: MEMS, Geophone, Accelerometer.

1 Introduction

Continuous research is going on to response to an earthquake accurately to avoid pseudo shut down of the plant such as calculation of cumulative absolute velocity is revised as standardized cumulative absolute velocity (CAV)[1]. But a well defined complete response to an earthquake event is still necessary for more availability of the plant confirming integrity of structure, system, and components (SSC). So, existing earthquake instrumentation and procedures should be reviewed and updated.

Seismic sensor is one of the most important components to design earthquake instrumentation for nuclear power plant. Traditional geophone, Servo Acceleration with Feedback Loop, Force Balanced Accelerometer (FBA), and Micro Electro Mechanical System (MEMS) are recognized seismic sensors for receiving earthquake information. This study develops a design of MEMS sensor based Earthquake Instrumentation consisting Field Programmable Gate Array (FPGA) seismic data processing system for quick assessment of the events comparing with design Operating Basis Earthquake (OBE) and Safe Shutdown Earthquake (SSE) levels of the plants. For completing research, a comparative study has been done among the various seismic sensors such as traditional geophone, servo acceleration with feedback loop, FBA, and MEMS. At first, the transfer functions of various sensors are elicited. Then, various curves such as magnitude, phase, and step response are extracted using MATLAB program. MEMS accelerometers can record to fractions of 1 Hz without any relative reduction in acceleration amplitudes. MEMS based digital accelerometers provide a broadband linear response (DC to 800 Hz) and very low distortion. In addition, various advantages of MEMS sensor are pointed out over traditional sensors by reviewing related documents.

We review the main operating characteristics such as sensitivity, full scale, dynamic range, noise, etc. of MEMS-based Digital Sensor Units (DSU), especially comparing with geophones, and discuss the quality and weight issues. We conclude that their use with an adapted high-density geometry makes it possible to

achieve much better data acquisition than with geophone arrays, for an equivalent cost. Various advantages over other sensors help us to select MEMS in earthquake instrumentation replacing traditional sensor. For this reason, MEMS based earthquake instrumentation containing FPGA seismic data processing system is designed and synthesized. It can provide automatic various parameter information such as OBE exceedance level comparing CAV threshold, SSE exceedance level comparing Peak Ground Acceleration (PGA) value, and Modified Mercalli Intensity (MMI) scale of the earthquake. This study will help to do quick assessment of the earthquake events and encourage updating the existing procedure to response to an earthquake event so that more availability of the plant can be ensured.

2 Methodology

2.1 Simulation of transfer function and comparative analysis of various seismic sensors

2.1.1 Basic architecture of sensors

Architecture of geophone and MEMS are shown in Fig. 1[2]. In Fig. 1, Geophone (left): the sensor casing (blue) is attached to a spike (grey) and to the magnet (yellow). These entire components move with ground motion, while the coil (red) connected to the casing by a soft

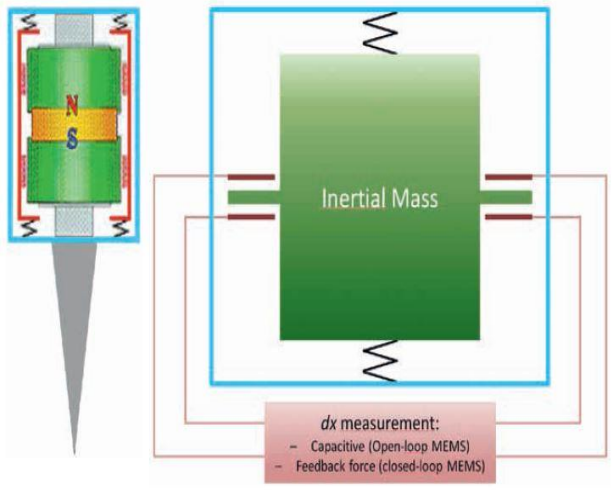

(a) (b)

Fig. 1 Architecture of (a) geophone (b) micro electro mechanical system (MEMS)

spring (black), remains motionless. Digital sensors (right): the principle is the same as for geophones on a microscopic scale, with a MEMS casing (blue) attached to a sensor casing (not represented). The inertial mass (green) is maintained by stiff springs (black) and then moves with casing/ground motions. When subjected to acceleration, the small displacements of the inertial mass are measured by electrodes (red)[2].

2.1.2 Traditional geophone in velocity domain

When ground motion frequency is equal to geophone natural frequency, it works in velocity domain and acts as a accelerometer. The free scale transfer function of traditional geophone in velocity domain (assuming earthquake angular frequency, $\omega \approx$ natural angular frequency of geophone, ω_0) is shown in equation (1)[3].

$$\frac{\omega^2}{(-\omega^2 + 2j\lambda\omega_0\omega + \omega_0^2)} \quad (1)$$

Considering, natural frequency, $f_0 = 10$ Hz, Damping Ratio, $\lambda = 0.7$, Transfer function using MATLAB program is shown in equation (2).

$$\frac{-0.0002533s^2}{0.0002533s^2 - 0.02228s - 1} \quad (2)$$

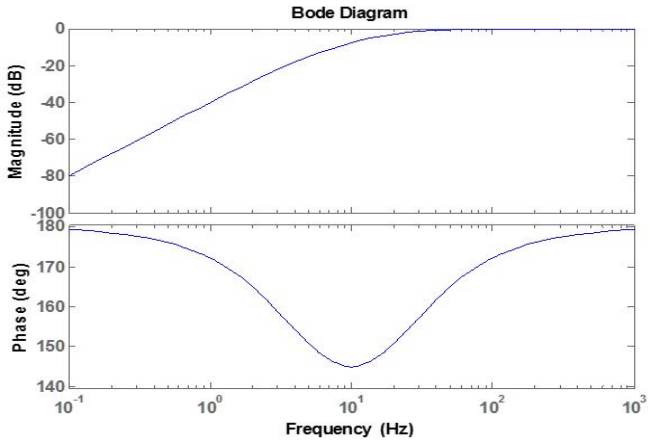

Fig. 2 Bode plot of magnitude and phase spectra of traditional geophone in velocity domain

2.1.3 Servo acceleration with feedback loop (AC-23)

The AC-23 provides over-damping the geophones with a feedback amplifier in a bridge circuit. The principle of over-damping geophones is done by applying a voltage on the geophone, which has opposite polarity from the voltage, which is induced by the moving geophone coil. Since the voltage

induced by the geophone coil is proportional to the velocity, the externally applied voltage is also proportional to it. This results in a current in the coil (~force), which is also proportional to the velocity and therefore is a "damping" current, or additional damping. Increasing this damping further will lead to a resulting output that is proportional to acceleration. The geophone is connected in a resistor bridge, driven by a feedback amplifier and an inverter, which apply the amplified bridge differential signal in opposite polarity[4]. The amplifier has a fixed gain that will define the bandwidth of the accelerometer. The gain G and output V_o are represented by Equations (3) and (4).

$$G = 1 + \frac{Z2}{Z1} \quad (3)$$

$$V_o = G.V_i = \left(1 + \frac{Z2}{Z1}\right).V_i \quad (4)$$

Fig. 3 shows the equivalent circuit for the linear servo balanced accelerometer[4].

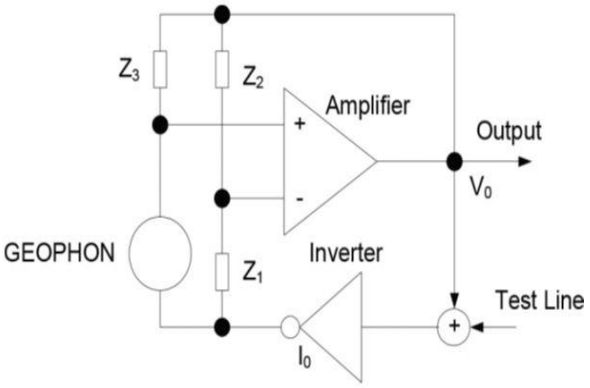

Fig. 3 Equivalent circuit for AC-23 (linear servo balanced accelerometer)

In Fig. 3, the test-line shifts the voltage to one side of the bridge, which produces a current flow in the geophone, resulting in a displacement step of the seismic mass. The movement of the mass generates a voltage across the Geophone, which is detected by the differential amplifier and induces an output signal. The effect of the test signal on the bridge is cancelled by the differential input of the amplifier. In this part, the Geophone transfer function is analysed in order to define how the sensor generates open-loop transfer function as depicted in Equation (3). The transfer function from MATLAB program is shown in equation (5)[4].

$$\frac{1.564s}{0.001251s^2 + 1.514s + 1} \quad (5)$$

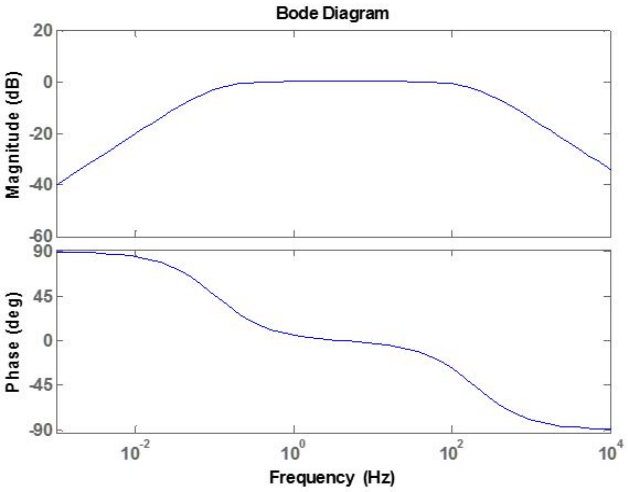

Fig. 4 Bode plot of magnitude and phase spectra of AC-23

2.1.4 Force balanced acceleration using pendulum

Kinemetrics Inc. Episensor Force Balance Accelerometer ES-T consists of three orthogonally mounted Force Balance Accelerometers (FBAs) – X-axis, Y-axis and Z-axis – inside a sensor casing. Each accelerometer module is identical and plugs into a board that provides the final output circuit and the carrier oscillator. The Fig. 5 below shows a simplified block diagram of the major components of each of the FBAs [5].

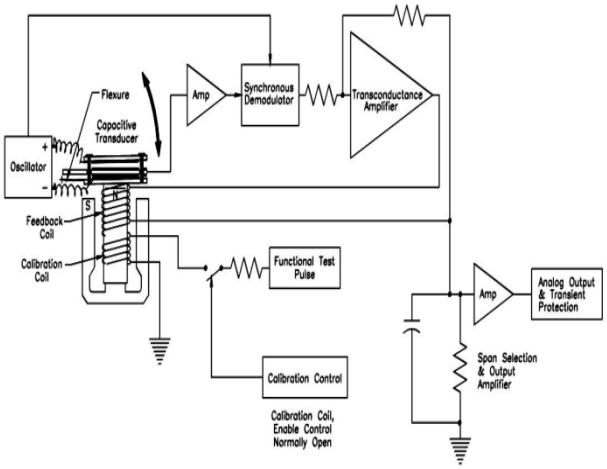

Fig. 5 Simplified block diagram of force balanced accelerometer

The transfer function of the sensor considering four poles is shown in equation (6)[5].

$$\frac{V(s)}{A(s)} = \frac{k_1 * k_2}{(s-p_1)(s-p_2)(s-p_3)(s-p_4)} \quad (6)$$

where, V(*s*) is Laplace transform of sensor output voltage in V, A(*s*) is Laplace transform of input acceleration either in **m/s^2** or in g, $k_1 = 2.46 \times 10^{13}$, k_2 =Semsitivity of the sensor in **V/g**, Here 2.5 **volt/g, s** is the Laplace transform variable. The poles are considered as[5]

p_1 = -981 + 1009i (Pole 1)
p_2 = -981 - 1009i (Pole 2)
p_3 = -3290 + 1263i (Pole 3)
p_4 = -3290 - 1263i (Pole 4)

Using MATLAB program, the transfer function is shown in equation (7).

$$\frac{2.5}{4.065e^{-014}s^4 + 3.472e^{-010}s^3 + 1.11e^{-006}s^2 + 0.00152s + 1} \quad (7)$$

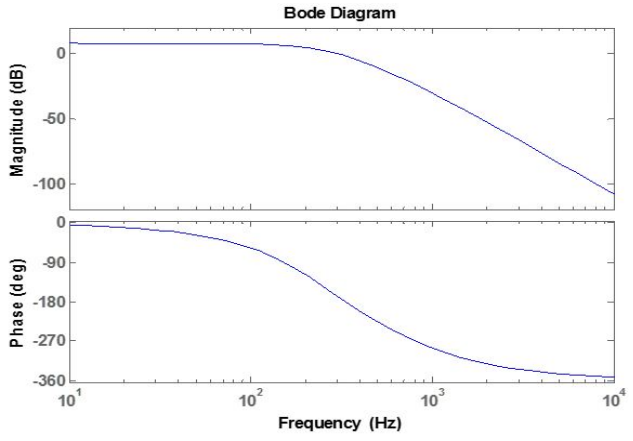

Fig. 6 Bode plot of magnitude and phase spectra of episensor FBA considering sensitivity and four poles

2.1.5 Traditional MEMS in acceleration domain

The free scale transfer function of traditional MEMS in acceleration domain (assuming $\omega << \omega_0$) is shown in equation (8)[3].

$$\frac{-1}{(-\omega^2 + 2j\lambda\omega_0\omega + \omega_0^2)} \quad (8)$$

Considering natural frequency, f_0=1000 Hz, Damping Ratio,λ=0.7 from MATLAB program, the tranfer function is shown in equation (9).

$$\frac{2.533e^{-008}}{2.533e^{-008}s^2 - 0.0002228s - 1} \quad (9)$$

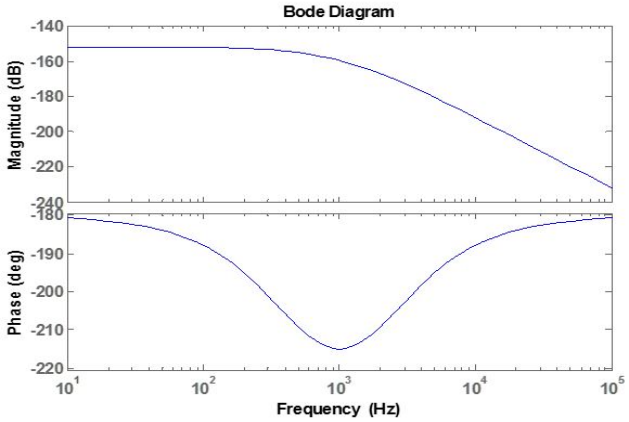

Fig. 7 Bode plot of magnitude and phase spectra of traditional MEMS

2.1.6 ADXL MEMS accelerometer with low pass filter

Equation (10) presents a generic, second-order model that presents an approximation for the mechanical portion of a MEMS accelerometer's response to frequency. In this model, f_0 represents the resonant frequency and Q represents the quality factor [6].

$$H_M(s) = \frac{\omega_0^2}{s^2 + (\omega_0/Q) \times s + \omega_0^2} \quad (10)$$

where, $f_0 = \frac{\omega_0}{2\pi}$

Some MEMS accelerometers use a single pole, low-pass filter to help lower the gain of the response at the resonant frequency. Equation (11) offers a generic model for the frequency response associated with this type of filter (H_{SC}). In this type of filter model, the cutoff frequency (f_C) represents the frequency at which the magnitude of the output signal is lower than its input signal by a factor of $\sqrt{2}$ [6].

$$H_{SC}(s) = \frac{\omega_C}{s + \omega_C} \quad (11)$$

where, $\omega_C = 2\pi f_C$

Equation (12) combines the contributions of the

mechanical structure (H_M) and the signal chain (H_{SC}).

$$H_T(s) = H_M(s) \times H_{SC}(s)$$

$$H_T(s) = \frac{{\omega_0}^2}{s^2 + (\omega_0/Q) \times s + {\omega_0}^2} \times \frac{\omega_C}{s+\omega_C} \qquad (12)$$

This model assumes a nominal resonant frequency of 1000 Hz, a Q of 17, and the use of a single-pole, low-pass filter that has a cutoff frequency of 1500 Hz. Using MATLAB program, the transfer function is shown in equation (13)

$$\frac{5.922e^{010}s}{s^3 + 1870s^2 + 4.003e^{007}s + 5.922e^{010}} \qquad (13)$$

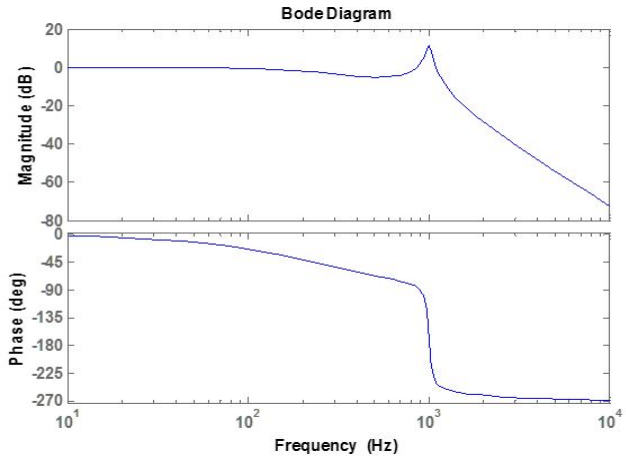

Fig. 8 Bode plot of magnitude and phase spectra of ADXL MEMS with low pass filter

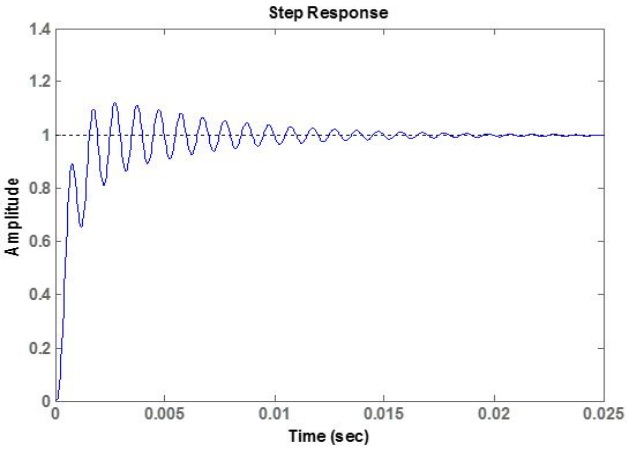

Fig. 9 Transfer function's step response of ADXL MEMS with low pass filter from MATLAB program

2.1.7 Comparative analysis

Geophones act as accelerometer at their resonant frequency (commonly 10 Hz) and deliver an analog voltage proportional to ground acceleration. Though traditional sensors which perform tremendous job in earthquake instrumentation, it suffer significant reduction in recorded velocity-domain amplitudes and below their natural frequency.

In Fig. 2, amplitude reduction is observed at the lower frequency. On the other hand a constant amplitude response is observed up to 100 Hz in case of force balanced accelerometer as shown Fig. 6. MEMS digital sensors act as accelerometers below their resonant frequency (around 1 kHz) and deliver digits proportionally to ground acceleration. MEMS sensor which is applied to our design has multidimensional advantage over traditional sensors. With low power consumption and full functionality at any tilt angle, the digital sensor unit has proven to be high-performance, power efficient and reliable in all operations. It digitizes data from a single ground location and its three orthogonal components allow it to accurately record the ground motion on all three axes. This is a significant improvement over analog sensors that only record the vertical component. The performance parameters such as noise floor, full scale, dynamic range, sensitivity, and data quality prove suitability of MEMS sensor over traditional geophone sensor[2][7][8]. The importance factors that the installation and maintenance cost of the MEMS are lower than other sensors.

MEMS response to acceleration is constant from frequency 0 Hz to 800 Hz, both in phase and in amplitude as shown in Fig. 7 and Fig. 8 which are optimal to capture a broadband signal[9]. So, MEMS sensor response is linear in the acceleration domain down to DC, there should be no attenuation and sufficient signal-to-noise ratio toward the low end of the spectrum**.** The latest version of MEMS shows less noise floor than geophone even in lower frequency as shown in Fig. 10[8]. MEMS sensor shows the best potentiality among various seismic sensors for digital data output which is essential for interfacing with Field Programmable Gate Array (FPGA). This

accelerates to design MEMS based earthquake instrumentation with FPGA data processing system for nuclear power plant.

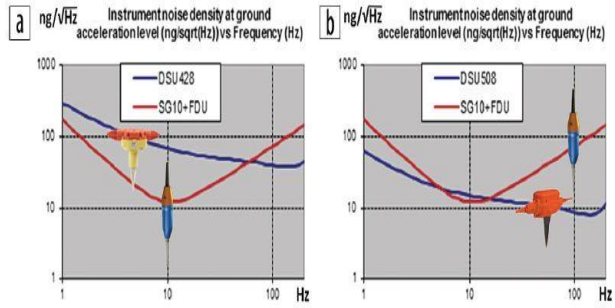

Fig. 10 Comparison in acceleration of the noise floor from different sensors: (a) previous-generation MEMS sensor and (b) the new one, both shown versus a 10-Hz geophone connected to a digitizer. The new MEMS brings the noise floor to a level lower than that of the geophone[8].

2.2 Conceptual design and synthesis

2.2.1 Design architecture

MEMS based earthquake instrumentation including FPGA data processing system for nuclear power plant is conceptually designed. Fig. 11 shows block diagram of the conceptual design.

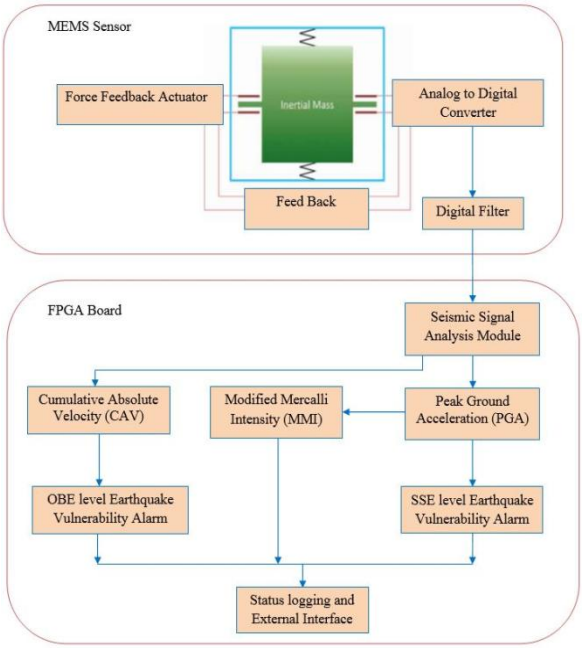

Fig. 11 Block diagram of MEMS based earthquake instrumentation with FPGA data processing system for nuclear power plant

2.2.2 Design synthesis

The cumulative absolute velocity value indicates whether the earthquake exceeds the Operating Basis Earthquake (OBE) level or not. If it reaches a threshold value, the event is considered as exceeded OBE level. Cumulative absolute velocity is standardized as[1].

$$\mathrm{CAV_{Total}} = \mathrm{CAV_i} + \int_{t_{i-1}}^{i} |\, a(t) \,|\, dt \qquad (14)$$

Where, a(t) = acceleration values in a one-second interval where at least one value exceeds 0.025g, i = 1, n with n equal to the record length in seconds. The revised CAV threshold is 0.16 g.s

Peak ground acceleration (PGA) is equal to the maximum ground acceleration that occurred during earthquake shaking at a location. PGA is equal to the amplitude of the largest absolute acceleration recorded on an accelerograph at a site during a particular earthquake. Peak ground acceleration is mathematically expressed as[10]

$$\mathrm{PGA} = \mathrm{Max}\{|a(t)|\} \qquad (15)$$

where, a(t) = acceleration value at time t.

The effect of an earthquake on the Earth's surface is called the intensity. The intensity scale consists of a series of certain key responses such as people awakening, movement of furniture, damage to chimneys, and finally – total destruction. Table 1 shows relationship between Modified Mercalli Intensity (MMI) scale and PGA[11].

Table 1 Relationship between MMI and PGA

MMI scale	PGA (g)
I	<0.0017
II – III	0.0017 – 0.014
IV	0.014 – 0.039
V	0.039 – 0.092
VI	0.092 – 0.18
VII	0.18 – 0.34
VIII	0.34 – 0.65
IX	0.65 – 1.24
X+	>1.24

Safe Shutdown Earthquake (SSE) also called Design Basis Earthquake (DBE) is the maximum earthquake

potential for which certain structures, systems, and components, important to safety, are designed to sustain and remain functional. Operating Basis Earthquake (OBE) is an earthquake that could be expected to affect the site of a nuclear reactor, but for which the plant's power production equipment is designed to remain functional without undue risk to public health and safety. There is established relation between design OBE and SSE level with PGA for nuclear power plant in South Korea. Table 2 shows the PGA values for OBE and SSE.

Table 2 PGA for OBE and SSE

Design Earthquake	PGA	
	Horizontal	Vertical
SSE for OPR1000	0.2g	0.13g
SSE for APR1400	0.3g	0.3g
OBE for OPR1000	0.1g	0.067g
OBE for APR1400	0.1g	0.1g

However, if PGA value exceed the predefined value as shown in Table 2, equipment and piping, as well as the structure itself, may have been exceeded operating basis and design base earthquake level. When Earthquake event exceed SSE level, long term evaluation is necessary which is time consuming. At this case, further evaluation of structure, system, components should be performed. The new system has easier data accessibility and ensures integrated decision making process. So, with low execution time and easy accessibility to multi-decision parameters (CAV, PGA, MMI, OBE and SSE Vulnerability alarm), the modified system can give quick and authentic parameter information to evaluate earthquake events.

3 Results and discussion

Though traditional sensors perform tremendous job in earthquake instrumentation, it suffer significant reduction in recorded velocity-domain amplitudes and below their natural frequency. But MEMS sensor shows constant amplitude response from DC (0 Hz) to its high resonance frequency (1000 Hz). With low power consumption and full functionality at any tilt angle, the digital sensor unit has proven to be high-performance, power efficient and reliable in all operations. It digitizes data from a single ground location and its three orthogonal components allow it to accurately record the ground motion on all three axes. This is a significant improvement over analog P-wave geophones that only record the vertical component. The performance parameters such as noise floor, full scale, dynamic range, sensitivity, and data quality prove suitability of MEMS sensor over traditional geophone sensor. The importance factors that the installation and maintenance cost of the MEME are lower than other sensor. The weight is half than geophone. The conceptual design containing MEMS sensor with FPGA data processing system is simple and has low execution time. For low weight, the MEMS sensor can be installed besides the various locations of the nuclear power plant such as safety class 1, 2, 3, and as well as non nuclear safety equipment. Its multi-decision parameters such as CAV can give OBE exceedance information. PGA can give SSE level exceedance information. Recent experience has demonstrated the need for guidance to nuclear plant owners and operators on the felt and/or measured at the site, but which have little or no potential for damage. Response to an earthquake for present and new design is shown in Fig. 12.

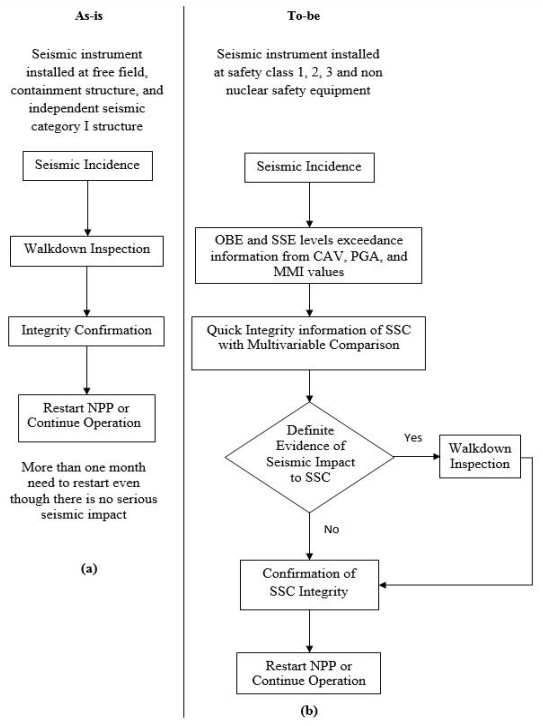

Fig. 12 Response to an earthquake (a) present earthquake response (b) earthquake response for new design

The modified system can reduce operator walkdown inspections load. Ground motion information recorded from various locations of the plant will be evaluated promptly after an earthquake as OBE and SSE can help to follow response procedures quickly with more clarity. Measurements of Effectiveness (MOE), Measurements of Performance (MOP), and Technical Performance Measures (TPM) of this work are listed in Table 3.

Table 3 MOE, MOP, and TPM

Criteria	Description
MOE	Low instrumentation cost, Availability of the plant, and Maintainability
MOP	Reduce Human Workload after the Seismic Incidence (for walk-down process), Automated decision making process for SSC integrity, Easy data accessibility
TPM	Low execution time, Handling multiple parameters, Quick assessment of the earthquake events

4 Conclusion

The absence of clear, detailed, and graded procedures for nuclear plant response to an earthquake may not only result in unnecessary shutdown but also their absence can be resulted as unnecessary inspections, tests and analyses of plant SSCs and make extensive delays in plant restart. The new system has low instrumentation cost. It is easily maintainable. With low execution time, it can ensure better availability of the plant through integrated decision making process by automatic assessment of nuclear power plant system, structure, and components. The study will be continued to acquire floor response spectrum from time history accelerograph for SSE level exceedance decision and the design will be implemented on FPGA platform in future.

Acknowledgement

This work was supported by the 2017 Research fund of the KEPCO International Nuclear Graduate School (KINGS), Republic of Korea.

References

[1] Yankee Atomic Electric Company, "Standardization of the Cumulative Absolute Velocity," EPRI, TR 100082, 1991.

[2] Nicolas Tellier and Jérôme Lainé, Understanding MEMS-based digital seismic sensors, FIRST BREAK, Volume 35, January 2017

[3] Michael S. Hons and Robert R. Stewart, Transfer functions of geophones and accelerometers and their effects on frequency content and wavelet, CREWES Research Report , Volume 18, 2006

[4] J. C. Jung, Earthquake Instrumentation, Earthquakes - Tectonics, Hazard and Risk Mitigation, INTECH, 2017, DOI: 10.5772/66215, https://www.intechopen.com/books/earthquakes-tectonics-hazard-and-risk-mitigation

[5] Kinemetrics, Inc., User's Guide, Episensor Force Balanced Accelerometer, Model FBA ES-T, Document 301900, Revision D, October 2005.

[6] Mark Looney, MEMS Vibration Monitoring: From Acceleration to Velocity, Analog Dialogue 51-06, June 2017

[7] M. Moreau (Sercel), J. Lainé (Sercel) & M. Serrut (Sercel), MEMS-based Accelerometers - The Quest for Low Frequencies and Weak Signals, We P04 06, 76th EAGE Conference & Exhibition, Amsterdam RAI, The Netherlands, 16-19 June, 2014.

[8] Jérôme Lainé and Denis Mougenot, A high-sensitivity MEMS-based accelerometer, THE LEADING EDGE, November 2014

[9] D. Mougenot, and N. Thorburn, 2004, MEMS-based 3C accelerometers for land seismic acquisition: Is it time?: The Leading Edge, 23, no. 3, 246–250, http://dx.doi.org/10.1190/1.1690897.

[10] Jack R. Benjaminand Associates Inc., 1988, A Criterion for Determining Exceedance of the Operating Basis Earthquake, Electric Power Research Institute, NP – 5930.

[11] D. J. Wald, V. Quitoriano, T. H. Heaton, Relationships between Peak Ground Acceleration, Peak Ground Velocity, and Modified Mercalli Intensity in California, Earthquake Spectra, vol. 15, no. 3, pp. 557-564, August 1999.